JOURNAL OF PHYSICAL ORGANIC CHEMISTRY
J. Phys. Org. Chem. 2007; **20:** 229–235
Published online 2 April 2007 in Wiley InterScience
(www.interscience.wiley.com) DOI: 10.1002/poc.1132

[5-(*p*-alkoxy)phenyl-10, 15, 20-tri-phenyl] porphyrin and their rare earth complex liquid crystalline

Miao Yu,[1]* Wen-yang Zhang,[2] Yong Fan,[1] Wen-ping Jian[1] and Guo-fa Liu[1]

[1]College of Chemistry, Jilin University, Changchun 130023, P.R. China
[2]College of Materials and Engineering, Jilin University, Changchun 130023, P.R. China

Received 13 July 2006; revised 21 September 2006; accepted 21 October 2006

ABSTRACT: Three series of porphyrin liquid crystalline compounds, [5-(*p*-alkoxy)phenyl-10, 15, 20-tri-phenyl] porphyrin and their rare earth complexes (Tb (III), Dy (III), Er (III), Yb (III)), with a hexagonal columnar discotic columnar(Col_h) phase have been synthesized. These compounds were characterized by elemental analysis, molar conductances, UV-visible spectra, infrared spectra, luminescence spectra, and cyclic voltammetry. These compounds exhibit more than one mesophases, which transition points of temperature change from −33.6 to 16.0 °C, and transition points of temperature for isotropic liquid also increase from 4.9 to 38.2 °C, with increasing chain length. Their surface photovoltage (SPV) response have also been investigated by the means of surface photovoltage spectroscopy (SPS) and field-induced surface photovoltage spectroscopy (EFISPS). It was found that their SPV bands are analogous with the UV-visible absorption spectra and derived from the same transition. Copyright © 2007 John Wiley & Sons, Ltd.

KEYWORDS: porphyrins; lanthanide; liquid crystals; cyclic voltammetry; SPS and EFISPS

INTRODUCTION

Porphyrins, as a model hemoglobin, myoglobin, and cytochrome P_{450}, have been widely studied, because of their interesting excited state, catalytic behavior, and ubiquitous electron-transfer processes.[1–4] While their transition metal complexes have been extensively investigated, fewer studies of rare earth porphyrin complexes have been reported comparatively. The work in this area is limited to specific NMR shift reagents, heavy atom probes for electron microscopy and X-ray structure determination, and agents for photodynamic therapy *et al*.[5–8] As we know, liquid crystalline system is the combination of the ordered structure of a crystal phase and the molecular mobility of an isotropic (liquid) phase, which allow liquid crystal mesophases to self-correct structural defects.[9–11] Thus, they can exhibit electric or magnetic responses and have potential application in the field of electronic devices, that is, information storage.[12–13] Porphyrins have been revealed to be a class of fascinating liquid crystalline materials due to their synthetic versatility, thermal stability, large π-electron system, and photochemical properties.[14] However, the studies on porphyrin liquid crystal compounds, as well as their rare earth porphyrin complexes have focused on a certain aspect property such as fluorescence, besides their liquid crystallinity. In our lab, extensive efforts have been to devoted this kind of porphyrins and their rare earth complexes, some good results have been reported.[15–17] In this paper, we synthesized three series of porphyrin liquid crystals whose structures are shown in Fig. 1, investigated their surface photovoltage spectra (SPS), electrochemical behavior, luminescence spectra, and liquid crystalline properties.

**Correspondence to:* M. Yu, College of chemistry, Jilin University, Changchun 130023, P.R. China.
E-mail: yumiao@jlu.edu.cn

RESULTS AND DISCUSSION

Luminescence spectra

Tables 1 and 2 give the excitation and emission spectral data of the ligands and complexes. The quantum yields (Φ_f) were calculated by the following equation:

$$\Phi_f = \frac{\Phi_{fs} \cdot n^2 \cdot A_s \cdot I_f}{n_s^2 \cdot A \cdot I_{fs}}$$

In the above equation, n_s, A_s, and I_{fs} represent the refractive index, absorbance, and integrated intensity of standard sample at excited wavelength, respectively. Meso-tetraphenylporphyrin zinc, ZnTPP was used as standard sample, $\Phi_{fs} = 0.033$.[18]

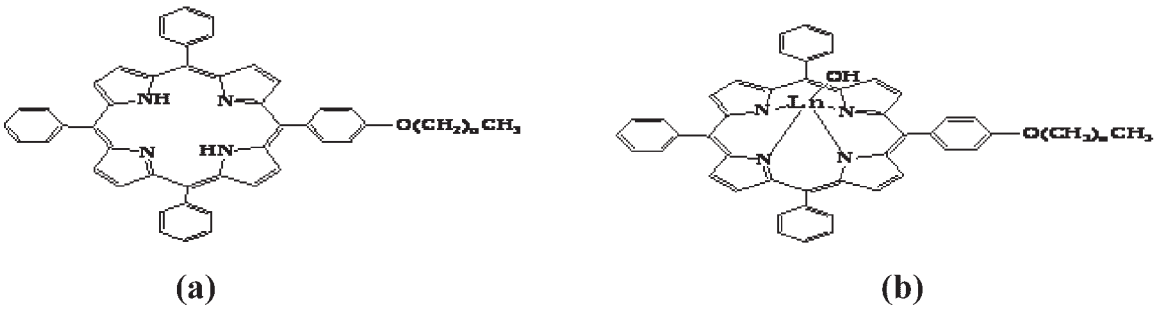

(a) (b)

Figure 1. Porphyrin liquid crystalline compounds: [5-(*p*-alkoxy)phenyl-10, 15, 20 -tri-phenyl]porphyrin(a), $n = 11$, 13, 15 correspond to 12L, 14L, 16L, respectively; [5-(*p*-alkoxy)phenyl-10, 15, 20-tri-phenyl] porphyrin lanthanide complex(b), n = 11, 13, 15; Ln = Yb, Er, Dy, Tb, correspond to 12ErOH, 12DyOH, 12TbOH, 14YbOH, 14ErOH, 14DyOH, 14TbOH, 16YbOH, 16ErOH, 16DyOH, 16TbOH, respectively

Two fluorescence bands S_2 (B, Soret band) and S_1 (Q band) are observed in porphyrin complexes, which are attributed to transition from the second excited singlet state S_2 to ground state S_0, $S_2 \rightarrow S_0$ and $S_1 \rightarrow S_0$ of Q band emission, respectively. The Soret fluorescence is about two orders of magnitude weaker than the $S_1 \rightarrow S_0$ of Q band emission. Its quantum yield is very low and sometimes, it becomes unobservable. In our experiment, this fluorescence emission can not be observed at room temperature at excited wavelength, 420 nm. Soret bands in three ligands and eight complexes are split into two bands, as compared with their UV-visible absorption spectra. Other spectral bands undergo only a small change. Q (0–0) fluorescence bands of the complexes are in the region 600–606 nm, while Q (0–1) fluorescence bands of the complexes in the region 651–655 nm and Q (0–2) bands 712–720 nm, see Fig. 2. They are mirror symmetric to the absorption spectra. Quantum yields (Φ_f) of Q band for the complexes are in the range 0.0007–0.2067 and ligands 0.09508–0.2098. Obviously, the quantum yields of complexes are much less than those of ligands.

As we know, the $S_1 \rightarrow S_0$ quantum yield depends on the relative rates of the radiative process $S_1 \rightarrow S_0$ and two radiationless processes $S_1 \rightsquigarrow S_0$ and $S_1 \rightsquigarrow$ Tn. According to the known result, the fluorescence quantum yields of the porphyrin complexes are low.[18] Therefore, in our experiment, because the spin forbidden process $S_1 \rightsquigarrow$ Tn plays a predominant role in radiation absent deactivation of S_1 in porphyrin complexes, the fluorescence quantum yields of complexes are much less than 0.21.[18]

Table 1. Excitation spectral data of ligands and complexes

Compounds	Peak values(λ per nm)				
12L	408	431	519	548	594
14L	405	431	518	549	593
16L	417	428	515	552	592
12YbOH	410	430	520	554	589
12ErOH	418	437	517	558	592
12DyOH	419		515	557	592
12TbOH	419		519	554	590
14YbOH	416	426	519	556	591
14ErOH	411	430	516	549	589
14DyOH	418	437	516	556	585
14TbOH	415	430	511	554	589
16YbOH	419		514	552	593
16ErOH	419		518	553	593
16DyOH	415	431	516	551	594
16TbOH	415	427	517	552	594

Surface photovoltaic spectroscopy (SPS) and electric field-induced surface photovoltaic spectroscopy (EFISPS)

The surface photovoltage spectroscopy technique, as a very sensitive characterization method to detect the change of charge distribution on functional semiconductor surfaces, is related to electron transition processes, caused by light absorption. So it can directly reflect the properties of photogenerated charge separation and

Table 2. Emission spectral data of ligands and complexes ($\lambda_{ex} = 420$ nm)

Compounds	Peak values (nm)			Quantum yields(Φ_f)
	Q(0–0)	Q(0–1)	Q(0–2)	
12L	604	653	717	0.1255
14L	605	653	716	0.09508
16L	603	654	712	0.2098
12YbOH	604	655	716	0.0008
12ErOH	604	651	718	0.0205
12DyOH	605	653	715	0.0308
12TbOH	603	652	720	0.0787
14YbOH	600	654	717	0.0172
14ErOH	606	654	716	0.0157
14DyOH	603	652	716	0.0261
14TbOH	603	653	716	0.0312
16YbOH	606	652	719	0.0740
16ErOH	606	652	713	0.2067
16DyOH	603	653	712	0.1409
16TbOH	603	653	718	0.0478

DOI: 10.1002/poc

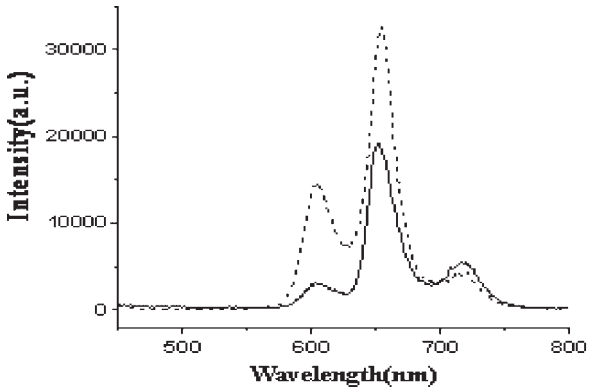

Figure 2. Emission spectra of 12L (. . . . . .) and 12TbOH (–) at room temperature in $CHCl_3$

charge transfer. Its sensitivity is up to 10^8 q cm^{-2}, or about one elementary charge per 10^7 surface atoms, increasing by several orders of magnitude, compared with the X-ray photoelectron spectroscopy.[19]

The SPS and EFISPS of the ligand 12L and its complex 12 ErOH are presented in Fig. 3. Their photovoltaic spectral bands are given in Table 3. The photovoltaic spectra of the ligand and complexes are similar to their UV-visible spectra, even the shape and the numbers of Soret and Q bands do not change. Therefore, it is deduced that the same electron transition processes occurred in both spectra.

Porphyrin molecule is a conjugated π bonding system, in which π-orbitals are analogous to energy band of organic semiconductor, and π^*-orbital to the conduction band. Photogenerated charge carriers in π system are nonlocalized, their motion is free in the valence band, the same as those photogenerated electrons in the conduction band. In this kind of system, the band to band transition is characterized as a π–π^* transition. The band at 300–400 nm is named as P band, corresponding to the higher energy level transition, $b_{2u}(\pi) \rightarrow e_g(\pi^*)$, while Q and Soret bands are due to $a_{2u}(\pi) \rightarrow e_g\ (\pi^*)$ and $a_{1u}\ (\pi) \rightarrow e_g\ (\pi^*)$ transitions, respectively.[20] The P band is transition from NHOMO (the next highest occupied molecular orbital) to LUMO (the lowest unoccupied molecular orbital), while the Q and Soret bands arised from the coupling of the two transitions between the HOMO (the highest occupied molecular orbital) and LUMO.[20]

By comparison of the spectral peaks of the 12L compound in Figs. 3(a) and (b), some change of 'simultaneous response' in the positive or negative electric field intensity was observed. The surface photovoltaic (SPV) response exhibits positive in positive electric field and negative in negative field. This kind of simultaneous response to the electric field can all be assigned to π–π^* transitions. However, the variation rates of Soret and Q bands, with an increase in the positive or negative electric field intensity are noticeably different. Since the common upper energy level transition in the π system is $\pi^*(e_g)$, the difference mainly stems from the lower energy levels. Briefly, the lower energy levels of these transitions are at different depths of the valence band, resulting in different photogenerated hole diffusion lengths. The response of the Q band is induced to a positive electric field. When employed in a negative electric field, the photogenerated electrons in the conduction band diffuse towards the bulks, thus, increase the probability of recombination with photogenerated holes, whereas diffusion lengths are shortened, leading to decreasing of the SPV response, even reversal. Comparing the SPS and EFISPS of 12L and 12ErOH, it is found that the SPV response of 12ErOH is different from that of the free ligand 12L, which shows the decrease of the peaks. Symmetric increase of the complexes is supposed to cause this phenomenon. In the meantime, the photovoltaic action spectra follow the absorption spectra response well, indicating that they are derived from the similar electron transition process.

Liquid crystals

Small-angle X-ray diffractions of 16L and 16DyOH have been measured at room temperature. The *d*-spacing of

Table 3. Spectral bands of SPS and EFISPS of the compounds

		Maximum peaks(λ_{max} per nm)					
Compounds	External field voltage(V)	P band	Soret(B) band	Q band			
12L	0	326	430	516	550	595	649
	0.0313	328	429	518	552	591	649
	0.0625	330	428	516	551	591	652
	0.125	332	429	519	550	591	651
	−0.0313	328	425	520	547	592	650
	−0.0625	324	430	517	551	588	652
	−0.125	326	428	518	552	592	652
12ErOH	0	364	424		552	588	
	0.125	363	425		548	580	
	0.25	362	424	518	551	589	
	−0.125	362	425	518	553	583	
	−0.25	360	423	518	550	583	

DOI: 10.1002/poc

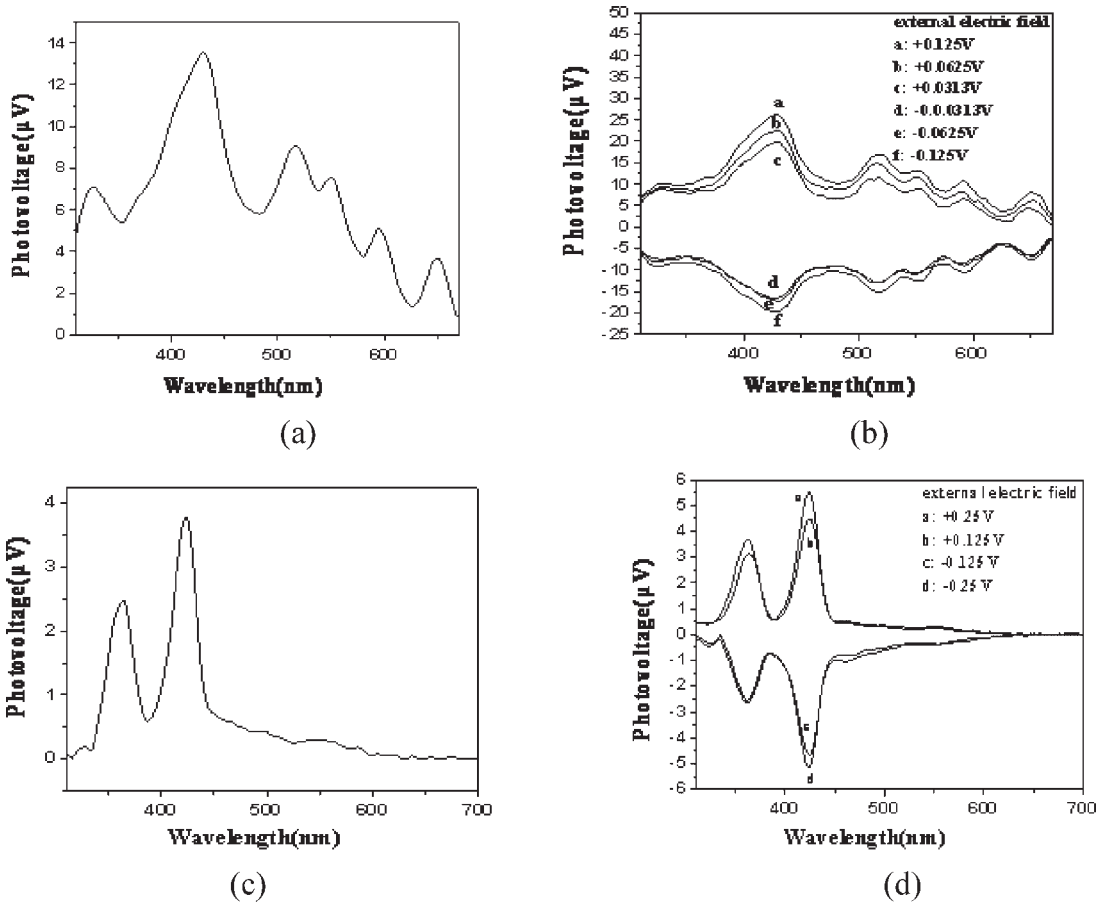

Figure 3. SPS and EFISPS of 12L and 12ErOH (a): SPS of 12L (b): EFISPS of 12L (c): SPS of 12ErOH (d): EFISPS of 12ErOH

16L are $d_{100} = 45.5$ Å, $d_{110} = 38.4$ Å, and $d_{200} = 23.0$ Å, respectively, while those of 16DyOH are 45.3, 27.1 and 22.6 Å. The ratios of the *d*-spacing, $1:1/\sqrt{3}:1/2$, are characteristic of a hexagonal columnar phase (Col_h). Their wide-angle X-ray diffraction both gave a broad peak, each centered at $2\theta = 20^\circ$, which is derived from the molten alkyl chains. The X-ray diffraction results of other compounds are similar to those of 16L and 16DyOH.

The transition temperatures and enthalpies of the porphyrin ligands and their complexes are given in Table 4. The liquid crystalline phase of all compounds were characterized by differential scanning calorimetry (DSC) and the optical texture was observed by viewing the birefringence of the sample between crossed polarizers in a polarizing microscope. The DSC data of complexes are summarized in Fig. 4. Figure 5 shows the birefringence texture for 16TbOH and 16L. From Table 4 and Fig. 4, more than one mesophases were found in these compounds. The complexes exhibited a systematic variety in their liquid crystalline, that is, the transition points of temperature tend to room temperature with increasing chain length (from $-33.6\,^\circ$C for 12ErOH to $16.0\,^\circ$C for 16YbOH), and the transition points of temperature for isotropic liquid increase with increasing chain length (from $4.9\,^\circ$C for 12ErOH to $38.2\,^\circ$C for 16TbOH). This advantage may have potential application for this kind of porphyrin crystalline liquids in the future.

EXPERIMENTAL SECTION

General methods

Infrared spectra were recorded on a Nicolet 5PC-FT-IR spectrometer, using KBr pellets in the region 400–4000 cm^{-1}. UV-visible spectra were recorded on a Shimadzu UV-240 spectrophotometer in the range 350–700 nm using chloroform as solvent. ^{1}H NMR spectra were recorded in deuterated chloroform using a Varian-Unity-400 NMR spectrometer and employing tetramethylsilane (TMS) as internal reference. Molar conductances of 10^{-3}mol dm^{-3} chloroform solution, at $25\,^\circ$C were measured on a DDX-111A conductometer. Elementary analysis was measured by a Perkin-Elmer 240C auto elementary analyzer. Optical microscopical properties were observed by a XinTian XP1 (CCD: TOTA-500 II) polarized light microscope, equipped with a variable temperature stage (Linkam TMS 94). Transition temperatures and heats of fusion were

DOI: 10.1002/poc

Table 4. Phase transition temperatures and enthalpy change of the porphyrin compounds

Compounds	$\xrightarrow[\Delta H/(kJ/mol)]{T/°C^a}$
12L	$C^b \xrightarrow[1.1]{-31.5} D^c \xrightarrow[24.1]{-15.5} I^d$
14L	$C \xrightarrow[0.9]{-9.7} D_1 \xrightarrow[0.4]{-1.7} D_2 \xrightarrow[20.7]{-4.3} D_3 \xrightarrow[1.9]{20.5} I$
16L	$C \xrightarrow[0.4]{-4.5} D_1 \xrightarrow[5.4]{4.2} D_2 \xrightarrow[24.1]{17.3} D_3 \xrightarrow[1.6]{31.0} I$
12ErOH	$C \xrightarrow[10.7]{-33.6} D_1 \xrightarrow[19.2]{-18.1} D_2 \xrightarrow[48.6]{4.9} I$
12DyOH	$C \xrightarrow[26.9]{-26.1} D \xrightarrow[38.8]{10.7} I$
12TbOH	$C \xrightarrow[21.5]{-25.3} D \xrightarrow[1.5]{20.3} I$
14YbOH	$C \xrightarrow[16.0]{-7.5} D_1 \xrightarrow[2.6]{7.1} D_2 \xrightarrow[0.8]{19.3} D_3 \xrightarrow[1.5]{25.1} I$
14ErOH	$C \xrightarrow[30.0]{-3.7} D_1 \xrightarrow[7.6]{6.9} D_2 \xrightarrow[10.8]{16.9} I$
14DyOH	$C \xrightarrow[3.2]{-11.1} D_1 \xrightarrow[1.7]{18.3} D_2 \xrightarrow[15.1]{26.5} I$
14TbOH	$C \xrightarrow[4.1]{-8.3} D_1 \xrightarrow[1.6]{3.5} D_2 \xrightarrow[0.8]{15.1} D_3 \xrightarrow[0.2]{32.5} I$
16YbOH	$C \xrightarrow[45.7]{16.0} D \xrightarrow[15.2]{35.4} I$
16ErOH	$C \xrightarrow[2.7]{14.9} D_1 \xrightarrow[2.9]{18.6} D_2 \xrightarrow[12.1]{30.8} I$
16TbOH	$C \xrightarrow[9.9]{12.4} D_1 \xrightarrow[9.1]{28.8} D_2 \xrightarrow[0.4]{38.2} I$

[a] Heating rate 10 °C min^{-1}. [b] C = crystal. [c] D = discotic mesophase. [d] I = isotropic liquid.

determined at scan rates of 10 °C min^{-1} by DSC, using a NETESCH DSC 204. Fluorescence spectra at room temperature in the region 300–800 nm, using 10^{-5} mol dm^{-3} chloroform as solvent were measured by FS920 Steady State Fluorescence Spectrometer. Excitation wavelength is at 420 nm. X-ray diffraction was recorded by a Shimadzu XRD-6000. Redox potentials of the porphyrins (10^{-3} M) in dried DMF, containing 0.1 M TBAP as a supporting electrolyte was determined at room temperature by cyclic voltammetry, using a three-electrode system under deaerated conditions and a CHI 600A electrochemical analyzer. Surface photovoltage spectroscopy was measured with a solid junction photovoltaic cell (ITO/Sample/ITO), using a light source-monochromator-lock-in detection technique. All reagents and solvent were of commercial

DOI: 10.1002/poc

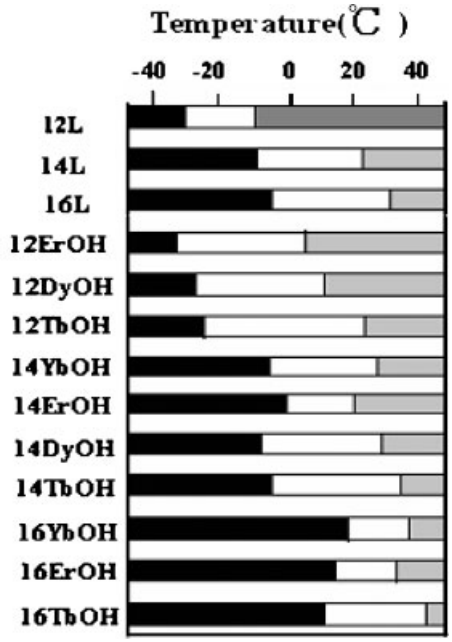

Figure 4. Differential scanning calorimetry of ligands and compounds. Black, solid phase; white, mesophase; gray, isotropic

reagent grade and were used without further purification except DMF and CH_3CN. DMF was pre-dried over activated 4 Å molecular sieves and vacuum distilled from calcium hydride (CaH_2), prior to use. The dry CH_3CN was obtained by re-distillation from CaH_2 in a glovebox.

Preparation of compounds

16L. [5-(*P*-hydroxy)phenyl-10, 15, 20-tri-phenyl]porphyrin (HPTPP) was prepared by general procedure.[21] The HPTPP (500 mg, 0.8 mmol) and 1-bromohexadecane (1221 mg, 4 mmol) were heated in a DMF, under the protection and stirred by a dry nitrogen stream for 2.5 h. The crude product was purified by column chromatography (silica gel, $CHCl_3$). The title compound was obtained as a purple solid (560 mg, 0.6 mmol, yield 82%). UV/vis ($CHCl_3$) ($10^{-4}\,\varepsilon\,M^{-1}\,cm^{-1}$): 419 (10.2), 516 (0.40), 551 (0.28), 590 (0.20), 647 (0.15) nm; IR (KBr): 3313, 2927, 2855, 1581, 1467, 1349, 1250, 978 cm^{-1}; *Anal. Calcd.* for $C_{60}N_4H_{62}O$: C 84.31, H 7.26, N 6.56, Found: C 84.39, H 7.20, N 6.61. Molar conductance value (MCV) ($CHCl_3$, 25 °C, $\Omega^{-1}\,cm^2\,mol^{-1}$): 0.14 (nonelectrolyte).[12] UV-visible in $CHCl_3$, 20 °C, λ_{max}/nm [lg (ε/$dm^3\,mol^{-1}\,cm^{-1}$) in parentheses]: 419 (5.00), 516 (3.59), 551 (3.34), 590 (3.25), 647 (3.17). ^1H NMR: 8.89 ppm, 8H, pyrrole ring; 7.26–8.22 ppm, 19H, meso-phenyl protons; −2.78, ppm N—H; 0.89–0.87 ppm, 3H, CH_3; 1.26–1.98 ppm, 28H, CH_2; 3.64–3.39 ppm, 2*H*, CH_2.

16TbOH. A mixture of 16L (300 mg, 0.35 mmol) and $TbCl_3{\cdot}6H_2O$ (262 mg, 0.7 mmol) in imidazole (1.0×10^4 mg) was heated at 210 °C, under the protection and stirred by a dry nitrogen stream for 2 h. The extent of the reaction was monitored by measuring the UV-visible spectra of the reaction solution at 10 min intervals. After cooling the reaction mixture to 100 °C, 150 ml distilled water was added, 200 ml chloroform was then added. The solution was shaken with 100 ml 0.1% aqueous $AgNO_3$, until no obvious AgCl was observed. The mixture was purified by column chromatography (neutral aluminum oxide, ethanol). The title compound was obtained as a purple solid (306 mg, 0.3 mmol, and yield 85%). UV/vis ($CHCl_3$, $10^{-4}\,\varepsilon\,M^{-1}\,cm^{-1}$) 423 (14), 516 (0.6), 551 (1.0), 591 (0.6) nm; IR (KBr): 3432, 2925, 2580, 1575, 1466, 1078, 1329, 1243 cm^{-1}, *Anal. Calcd.* for $TbC_{60}N_4H_{61}O_2$: C 70.00, H 5.93, N 5.44, Found: C 69.96, H 5.92, N 5.45. Molar conductance value (MCV) ($CHCl_3$, 25 °C, $\Omega^{-1}\,cm^2\,mol^{-1}$) 0.080 (nonelectrolyte). UV-visible in $CHCl_3$, 20 °C, λ_{max}/nm [lg (ε/$dm^3\,mol^{-1}\,cm^{-1}$) in parentheses]: 423 (5.15), 516 (3.76), 551 (3.99), 591 (3.78). ^1H NMR ($CDCl_3$): 8.8 ppm, 8H, pyrrole ring; 7.27 ppm, 19H, meso-phenyl protons; 0.76–0.89 ppm,

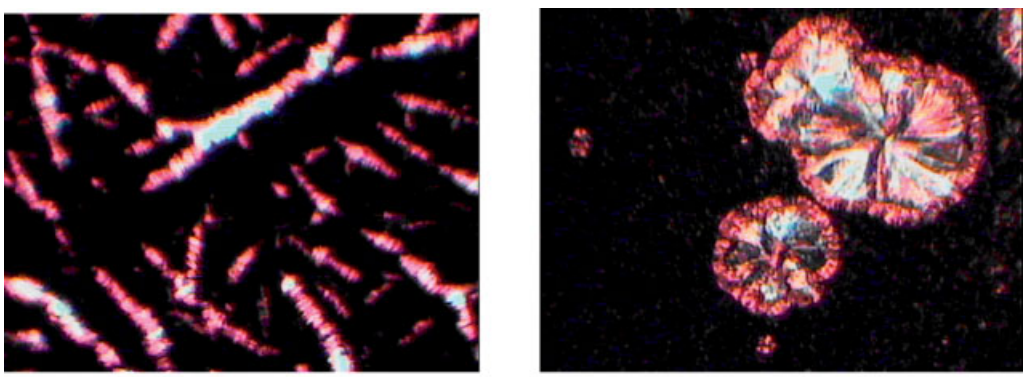

Figure 5. Optical texture of (a) 16TbOH at 37.9 °C and (b) 16L at 20.3 °C

DOI: 10.1002/poc

3H, CH_3; 1.24–1.80 ppm, 28H, CH_2; 4.09 ppm, 2*H*, CH_2; 0.20 ppm, 1H, —OH.

There are similar preparation methods and results for the other lanthanide complexes.

The molar conductance values of the ligand 12L and its complexes of 12YbOH, 12ErOH, 12DyOH, and 12TbOH are at 0.124, 0.018, 0.020, 0.048, and 0.076, respectively. Those of the ligand 14L and its corresponding complexes are at 0.129, 0.070, 0.072, 0.055, and 0.050, respectively. Those of the ligand 16L and its corresponding complexes are at 0.140, 0.028, 0.073, 0.048, and 0.080, respectively. It indicates that the ligands and all complexes show nonelectrolytic behavior.[22]

The porphyrin ligands 12L, 14L, 16L, and 14TbOH exhibited first and second reduction peaks are at $E_{1/2} = -1.582$, -2.094; -1.581, -2.076, and -1.580, -2.068 V *versus* Ag/Ag^+, respectively. The corresponding potentials for the porphyrin ring reaction in 14TbOH are at $E_{1/2} = -1.776$, -2.150 V *versus* Ag/Ag^+. Besides, the third reversible reduction of 14TbOH, concerning Tb^{3+} is at -1.345 V *versus* Ag/Ag^+. Obviously, the three porphyrin ligands 12L, 14L, and 16L exhibit two redox steps at close potentials, implying that the redox potentials do not change with the variation of the chain length ($n = 11$, 13, 15).

Acknowledgement

We thank the National Natural Science Foundation of China for financial support of this work.

REFERENCES

1. Seenisamy J, Bashyam S, Gokhale V, Vankayalapati H, Sun D, Siddiqui-Jain A, Streiner N, Shin-ya K, White E, Wilson WD, Hurley LH. *J. Am. Chem. Soc.* 2005; **127**: 2944–2959.
2. Gryko D, Li J, Diers JR, Roth KM, Bocian DF, Kuhr WG, Lindsey JS. *J. Mater. Chem.* 2001; **11**: 1162–1180.
3. Li J, Gryko D, Dabke RB, Diers JR, Bocian DF, Kuhr WG, Lindsey JS. *J. Org. Chem.* 2000; **65**: 7379–7390.
4. Schweikart K-H, Malinovskii VL, Diers JR, Yasseri AA, Bocian DF, Kuhr WG, Lindsey JS. *J. Mater. Chem.* 2002; **12**: 808–828.
5. Horrocks Dew W, Jr, Venteicher TF, Spilburg CA, Vallee BL. *Biochem. Biphys. Res. Commun.* 1975; **64**: 317–322.
6. Ramasseul R, Maldivi P, Marchon JC, Taylor M, Guillon D. *Liq. Cryst.* 1993; **13**: 729–733.
7. Chandrasekhar S. *Liq. Cryst.* 1993; **14**: 3–14.
8. Liu C–Y, Pan H–L, Fox MA, Bard AJ. *Science* 1993; **261**: 897–899.
9. Mody TD, Sessler JL. *J. Porphyrins Phthalocyanines* 2001; **5**: 134–142.
10. O'Neill M, Kelly SM, *Adv. Mater.* 2003; **15**: 1135–1146.
11. Kirsch P, Maillard D. *Eur. J. Org. Chem.* 2006; **15**: 3326–3331.
12. Bushby RJ, Lozman OR. *Curr. Opin. Solid State. Mater. Sci.* 2002; **6**: 569–578.
13. Hassheider T, Benning SA, Kitzerow H–S, Achard M-F, Bock. H. *Angew. Chem., Int. Ed.* 2001; **40**: 2060–2063.
14. Segade A, Castella M, Lo'pez-Calahorra F, Velasco D. *Chem. Mater.* 2005; **17**: 5366–5374.
15. Yu M, Liu GF, Cui XL. *J. porphyrin phthalocyanines* 2005; **9**(4): 231–239.
16. Yu M, Liu GF, Cheng YC, Xu WQ. *Liquid Crystals* 2005; **32**: 771–780.
17. Yu M, Liu GF, Zhao QD, Wang DJ, Jiang X. *Chinese J. Chem.* 2005; **23**: 1021–1026.
18. Quimby DJ, Longo FR. *J. Am. Chem. Soc.* 1975; **97**(8): 5111.
19. Zhao ZX, Xie TF, Liu GF. *Synthet. Metals* 2001; **123**(1): 33–38.
20. Gatos HC, Lagowski J, Banisch R. *Photogr. Sci. Eng.* 1982; **26**: 24–28.
21. Ji LN, Jia X. *Zhong Shan Da Xue Xue Bao* 1993; **32**(2): 1–8.
22. Wong CP, Horrocks Dew. W, Jr. *Tetrahedron Lett.* 1975; **16**(31): 2637–2640.

DOI: 10.1002/poc